Supersonic Plug Nozzle Design and Comparison to the Minimum Length Nozzle Configuration

Toufik Zebbiche* and ZineEddine Youbi*
Département d'Aéronautique, Faculté des Sciences de l'Ingénieur,
Université SAAD Dahleb de Blida, B.P. 270 Ouled Yaich, 09470 Blida, Algérie.

Abstract

A method to design the contour and conception of a plug nozzle of arbitrary shape, but specified exit flow conditions is presented. Severals shapes can be obtained for exit Mach number by changing the specific heats ratio. The characteristics of the nozzle in terms of length, weight and pressure force exerted on the wall are compared to the Minimum Length Nozzle and found to be better. Our field of study is limited to the supersonic mode to not to have the dissociation of the molecules. The design method is based on the use of the Prandtl Meyer function of a perfect gas. The flow is not axial at the throat, which may be advantageous for many propulsion applications. The performance benefits of the plug nozzle compared to the Minimum Length Nozzle are also presented.

Key Words : Supersonic Flow, Plug Nozzle, Prandtl Meyer Function, Design, Conception, Disctretization.

Nomenclature

θ	:	flow inclination angle.
M	:	Mach number.
γ	:	ratio of specific heats.
μ	:	angle of Mach.
φ	:	polar angle of Mach wave.
λ	:	polar ray of Mach wave.
x, y	:	cartesian coordinates.
Ψ	:	Angle inclination of the lip relative to the vertical.
ν	:	Prandtl Meyer function.
T	:	temperature.
P	:	static pressure.
ρ	:	density.
A	:	cross-sectional area.
t_M	:	thickness of material structural.
ρ_M	:	density of material of plug nozzle.
L	:	length of nozzle.
x_{plug}	:	distance between exit section and lip.
Fx	:	axial pressure force exerted on the wall of central body.
ε	:	relative error of computation.
N	:	number of discretization points.
σ	:	interpolation coefficient of the pressure on a segment of the wall. We take $\sigma=0.5$.

* Researcher Associate
E-mail : z_toufik270169@yahoo.fr

α, β : angles at vertices A and i of triangle connecting points A, i and $i+1$, see Figure 6.
l : nozzle depth.
MLN : abreviation of Mninmum Length Nozzle.

Subscript

E : Exit
0 : stagnation condition.
$*$: throat condition.
i : index denoting node.
(i) : index denoting nozzle segment.

Introduction

In high-speed aerodynamics and propulsion applications, it is desirable to design propulsion systems that have both a minimum length and weight[2), 5)]. It is known that the weight of the nozzle comprises a large portion of the overall weight of a conventional, high-speed projectile[1), 2)]. It is thus of interest to minimize the weight of the nozzle, and then use these weight savings to either increase the weight of the payload for improved mission effectiveness or to increase the initial fuel volume for an increased duration of flight. One approach is to use a minimum length nozzle (MLN). However it is well known that the MLN has relatively poor propulsion. In the present work, we present the design of a plug nozzle with central body, see Figure 1, that has superior performances compared to the MLN configuration[1)-6)]. The shpe of the central body is obtained in a manner so as to yield, a parallel and uniform flow at the exit section[2), 5), 12)]. This nozzle design and conception is examined for different specific heat ratios so as to illustrate its application in blowers and rocket motors.

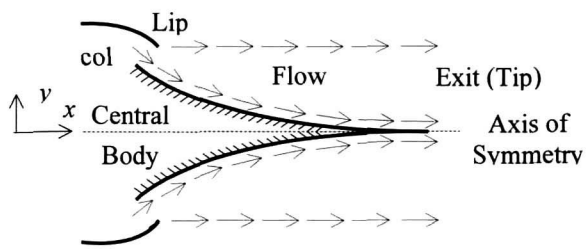

Fig. 1. Plug nozzle geometry

Refered 20) and 22) presents the first examination of the two-dimensional plug nozzle design for unknown contour. and the work in refered 21) extended by an examination of the effects when starting the flow. Refered 7), 8) and 16) present analyses of the supersonic flow in a plug nozzle of *a known contour.* In the present work we are interested in determining the design and conception of the nozzle for a specified exit flow. Refered 5), 9) and 15) compare different shapes of supersonic nozzles that are used for propulsion on rocket motors. A theoretical analysis modeling of the flow field in nozzles is presented in refered 10). The axisymmetric flow in a plug nozzle is examined in refered 13). Refered 14) examines the flow phenomena at the lip of the nozzle and considers it an analogouse to the flow at the trailing edge of wing profile. In refered 17), the flow in a plug nozzle is experimentaly examined, and their performance is found to be superior to other nozzles

types, in particular the *MLN* configuration. The plug nozzle design was first examined in refered 11). In this study, the primary focus was the design of central body that increased the nozzle's performance, in particular the propulsion power. In refered 12), the propulsive power of a plug nozzle was also examined, and the work in refered 11) extended by an examination of the effects when starting the flow. Although various numerical and analytical methods have been applied to the plug nozzles in these previous studies the geometry of the nozzle has been specified.

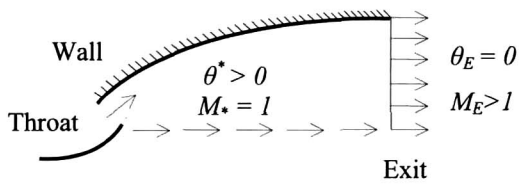

Fig. 2. Flow at the throat and the exit sections

In this present work, a numerical method for designing and sizing plug nozzle is presented. This method is based on the use of the Prandtl Meyer theory[1-22]. *The nozzle contour is unknown*; the desired contour is determined to give a parallel and uniform flow at the exit section, and also generate a maximum pressure force without losses since the flow is wholly axial at the exit. *It is noticed the Prandtl Meyer function present the base of all supersonic nozzle design.* The advantageous performance of the nozzle, in terms of the length, the mass of the structure and the force generated by the nozzle, are quantified by comparison with *MLN* configuration, which is widely used in aeronautical applications.

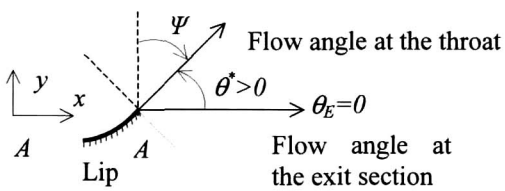

Fig. 3. Presentation of the angle Ψ

The plug nozzle consists of two parts, a convergent part and a divergent part that are joined to each other by a sonic throat. The present study focuses on the divergent part, since subsonic convergent part is used to simply give a sonic flow at the throat. A difference between the present model and the others that have been previously studied is that ***the flow at the throat is inclined at an angle θ^* compared to the nozzle axis*** as shown in Figure 2; in previous studies the flow is horizontal[9] at the throat. Consequently, the lip is inclined at an angle Ψ relative to the vertical as shown in Figure 3. The flow is permanent, two-dimensional, and irrotational. The design is limited to supersonic flows up to Mach number $M_E \leq 5.00$, such that there is no molecular dissociation. The streamline determined in the calculation is subsequently replaced by a rigid surface, which then represents the contour of the central body.

Mathematical formulation of the problem

The flow at the throat and the exit sections are one-dimensional. The ratio of the cross-sectional areas is used to compare the numerical calculations determined by our

model with the theory. The flow calculation inside the nozzle is rather delicate, since *the contour of the nozzle is unknown a priori.* The required contour of the central body is that which accelerates the flow from the Mach number $M=1.00$ at the throat up to the Mach number M_E at the exit section. As the flow angle is not zero at the throat, the flow angle deviation through the central body decreases only from $\theta=\theta^*$ at the throat to $\theta=0$ at the exit. The flow field and the contour central body determination are based on the Prandtl Meyer function presented by[1]:

$$\nu(M)=\left(\frac{\gamma+1}{\gamma-1}\right)^{1/2}\text{arctg}\left[\left(\frac{\gamma-1}{\gamma+1}\right)(M^2-1)\right]^{1/2}-\text{arctg}[M^2-1]^{1/2} \tag{1}$$

The angle ν is measured relative to the velocity vector at the throat.

In the Figure 4, the lines AB and AE respectively represent the Mach waves at the throat and the exit sections. These lines are inclined at the angles μ_B and μ_E with respect to the flow directions, and are given as $\mu_B=90$ *degree* and $\mu_E=arcsin[1/M_E] < 90$ *degree.*

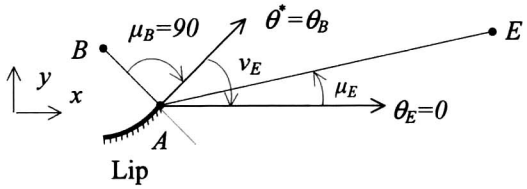

Fig. 4. Mach angles at the throat and exit sections

Between these two Mach lines, there is infinite number of Mach waves, centered on point A as shown in Figure 5. Along each Mach wave, the Mach number can be determined from which a point on the wall of the central body can be determined. Since the gas is perfect, the velocity vector is tangential to the streamline, which is the wall of the desired central body.

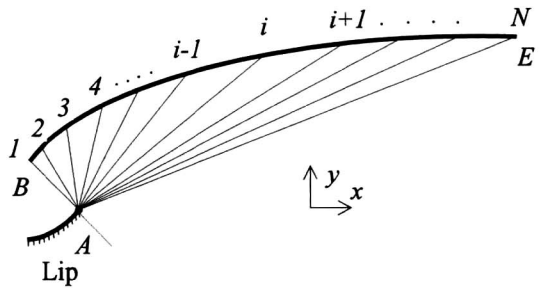

Fig. 5. Discretisation in the expansion zone

The flow properties, including Mach number, flow deviation, and thermodynamics ratios (pressure, temperature and density) are constant along each Mach line[2] that is centered on the point *A*. Figure 6 shows the parameters along an intermediate Mach line connecting points *A* and *i*. The angle θ_B is unknown a priori. However, to have a parallel and uniform flow at the exit section, it is necessary to incline the flow at the throat by an angle θ_B given by:

$$\theta_B=\nu_E=\nu(M_E) \tag{2}$$

The slope of the lip relative to the vertical is given by:

$$\Psi = (\pi / 2) - \nu_E \tag{3}$$

Discretization

The expansion zone between the lines AB and AE can be discretized into N Mach waves, including the two ends, as shown in Figure 5. Noting here that the Mach waves are straight lines.

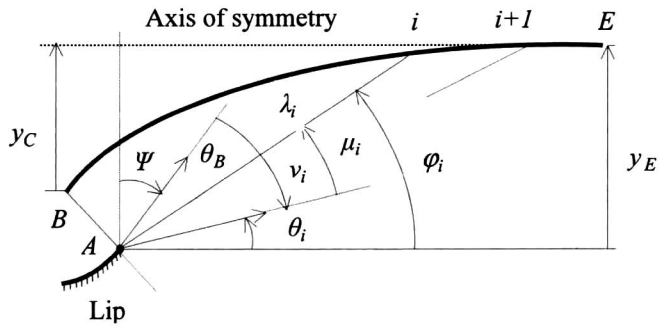

Fig. 6. Parameters of an intermediate Mach line connecting the points *A* and *i (i=2, 3, ..., N)*

The nozzle design is facilitated by discretizing the Mach number $1.00 \leq M \leq M_E$ into N values *so that calculations can be rapidly performed* as illustrated in Figure 6. Once the Mach number M_i at the point i is known then:

$$\mu_i = \arcsin(1 / M_i) \tag{4}$$

$$\nu_i = \nu(M_i) \tag{5}$$

$$\varphi_i = (\pi / 2) - \Psi - \nu_i + \mu_i \tag{6}$$

$$\theta_i = \varphi_i - \mu_i \tag{7}$$

In the Figure 6, the properties M_i, θ_i, ν_i, x_i, and y_i at the point i are known, and the problem then becomes the determination of these properties at the point $i+1$. On the triangle connecting the points A, i and $i+1$, we can write:

$$\alpha = \pi - \varphi_i + \nu_E - \nu_i \tag{8}$$

$$\beta = \varphi_{i+1} - \nu_E + \nu_i \tag{9}$$

$$\lambda_{i+1} / \lambda_B = (\lambda_i / \lambda_B) \sin(\alpha) / \sin(\beta) \tag{10}$$

By analogy with Eqs. (4), (5), (6), and (7), we can deduce those for the point $i+1$ by changing the index i by i+1. At this point, the Mach number M_{i+1} is known. The position of the point $i+1$, *in non-dimensional form,* is given by:

$$x_{i+1} / \lambda_B = (\lambda_{i+1} / \lambda_B) \cos(\varphi_{i+1}) \tag{11}$$

$$y_{i+1} / \lambda_B = (\lambda_{i+1} / \lambda_B) \sin(\varphi_{i+1}) \tag{12}$$

Calculation procedure

The first stage consists of the determination of some necessary results for the design: For a perfect gas, the critical thermodynamic ratios T_*/T_0, ρ_*/ρ_0, and P_*/P_0 are presented in refered 1).

The thermodynamics ratios T_E/T_0, ρ_E/ρ_0, and P_E/P_0 of a perfect gas corresponding to the exit Mach number are presented again in refered 1).

The theoretical ratio of critical sections is given by the following relation[3]:

$$A_E/A_* = M_E^{-1}\left((\gamma+1)^{-1}\left[1+(\gamma-1)/2\ M_E^2\right]\right)^{(\gamma+1)/[2(\gamma-1)]} \tag{13}$$

This ratio is also used as the basis of *comparison for validating our numerical calculations.*

The value ν_E of the Prandtl Meyer function is given by Eq.(2)

The slope of the lip compared to the vertical is given by Eq.(3)

As the calculation procerdure uses two successive points, it is necessary to initialize the calculation procedure. The starting point is point B. At this point, we have:

- The Mach number is $M_B = 1.00$. Sonic condition.
- The angle of Mach is $\mu_B = \pi/2$.
- The value of Prandtl Meyer function is $\nu_B = 0.0$.
- The polar angle is $\varphi_B = \pi/2 - \Psi - \nu_B + \mu_B$.
- The polar radius is $\lambda_B = 1.00$.
- The position of the first point of the wall is given, in the non-dimensional form, as:

$$x_B/\lambda_B = \cos(\varphi_B) \tag{14}$$

$$y_B/\lambda_B = \sin(\varphi_B) \tag{15}$$

- The flow angle deviation at the throat is given by:

$$\theta^* = \theta_B = \varphi_B - \mu_B \tag{16}$$

. The theoretical non-dimensional radius at the exit section is given using Eqs. (13) and (15) by:

$$y_E/\lambda_B = A_E/A_* \tag{17}$$

The second stage of calculation procedure is to assign the results of the point B to the first point of the numerical calculation, $i=1$.

Since the expansion region is discretized into N points, we then have $N-1$ panels, and thus, the Mach number at the point i $(i=1, 2, \ldots, N)$ is given by:

$$M_i = 1 + (i-1)\left[(M_E-1)/(N-1)\right] \tag{18}$$

Thus the thermodynamic and physical properties along all the selected Mach lines can be determined, and the contour of the central body is thus obtained.

At the last point, the following results apply:

- The position of the point E is given in non-dimensional form as:

$$x_E/\lambda_B = x_N/\lambda_B \tag{19}$$

$$y_E/\lambda_B = y_N/\lambda_B \tag{20}$$

- The axial distance between the exit section and the lip (point A) is given by:

$$x_{Plug} / \lambda_B = x_E / \lambda_B \tag{21}$$

- The length of nozzle is measured as an axial distance between the point B of the throat and the point E of the exit section. It is given in non-dimensional form by:

$$L / \lambda_B = (x_E / \lambda_B) - (x_B / \lambda_B) \tag{22}$$

- The ratio of cross-sectional areas corresponding to the descretization of N point is:

$$A_E / A_* \, (computed) = y_E / \lambda_B = y_N / \lambda_B \tag{23}$$

Thermodynamics Parameters

At each point i along the wall, the thermodynamic ratios can be determined from the isentropic relations[3]:

The temperature ratio is used to choose a suitable material of the central body. The density ratio helps us to evaluate the mass of the gas at each section along the central body flow, and the pressure ratio is used to determine the pressure force exerted on the wall.

Mass of the structure of the central body

The segment number *(i)* of the wall is illustrated in Figure 7. To calculate the mass of the central body, the following assumptions are made:

- The shape of the wall between two successive points is approximated by a straight of line.
- The central body is made up of the same material, and with a constant thickness.

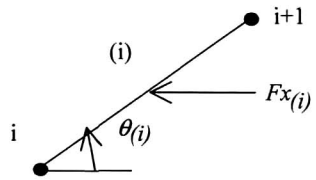

Fig. 7. Segment of a Plug nozzle

Thus the mass structure per unit depth and in non-dimensional form is:

$$Mass / (\rho_M \, t_M \, A_*) = C_{Mass} = \sum_{i=1}^{i=N-1} [(x_{i+1}/\lambda_B - x_i/\lambda_B)^2 + (y_{i+1}/\lambda_B - y_i/\lambda_B)^2]^{1/2} \tag{24}$$

Pressure force exerted on the wall

The pressure force exerted no a panel of Figure 7 is approximated by the following interpolation:

$$P_{(i)} = \sigma_i + (1-\sigma) \, P_{i+1} \tag{25}$$

The axial pressure force exerted on this panel is thus:

$$Fx_{(i)} = P_{(i)} \, (y_{i+1} - y_i) \, l \tag{26}$$

The axial pressure force exerted on the central body, per unit depth, is calculated as the sum of all the axial pressure forces exerted on all panels. In non-dimensional form thus have:

$$Fx / (P_0 A_*) = C_F = \sum_{i=1}^{i=N-1} (P / P_0)_{(i)} (y_{i+1} / \lambda_B - y_i / \lambda_B) \tag{27}$$

Mass of the gas in the divergent part of the nozzle

The mass of the gas in the divergent part of the central body between the Mach lines AB and AE including the uniform zone, assuming that the density is uniform in triangular region with vertices A, i and $i+1$, where for each triangular region is approximated by:

$$Mass_{Gas\,(i)} = \rho_{(i)} A_{(i)} l \tag{28}$$

with

$$\rho_{(i)} = (\rho_i + \rho_{i+1}) / 2 \tag{29}$$

$$A_{(i)} = (x_{i+1} y_i - x_i y_{i+1}) / 2 \tag{30}$$

In the uniform zone, the mass of the gas, per unit depth, is given by

$$Mass_{Gas}(uniform\ zone) = \rho_E (x_E y_E) / 2\ l \tag{31}$$

The total mass of the gas in the devergent section including the symmetry of the central body, per unit depth, will thus be given, in non-dimensional form, by the following relation:

$$Mass_{Gaz} / (\rho_0 \lambda_B^2 l) = C_{Gas} = (\rho_E / \rho_0)[(x_E / \lambda_B)(y_E / \lambda_B)] + \sum_{i=1}^{i=N-1} \left[\frac{\rho}{\rho_0}\right]_{(i)} [(x_{i+1} / \lambda_B)(y_i / \lambda_B) - (x_i / \lambda_B)(y_{i+1} / \lambda_B)] \tag{32}$$

Results and comments

Results are presented for three values of the specific heats ratio $\gamma = 1.30,\ 1.40,$ and $5/3$. The contour of the central body is presented in terms of non-dimensional axes.

The design results such as the central body length, the mass of the structure, the pressure force, the mass of the gas presented respectively by Eqs. (22), (24), (27), and (32) are presented *in non-dimensional form*.

Effect of the discretization on the convergence of the problem

If we increase the discretization number N of points, we can see the convergence of the numerical results towards the exact solution. We can take for instance $M_E = 2.50$, $\lambda_B = 1.0$ and $\gamma = 1.40$.

The theoretical ratio of cross-sectional areas is given by $A_B/A_* = 2.6367188$. The results presented in table 1 depend not on the discretization. We note here that $\Psi + \theta^* = 90°$. Table 2 presents various numerical results obtained from the design parameters of the suggested example versus the number N of points. The problem is convergent with a given relative error ε, if the sections ratio numerically calculated for a discretization and the theoretical sections ratio check the relation (33). The parameters also converge towards the precise solution.

Table 1. Design Parameters of the suggested exemple not depend on the discretizaton

$\Psi(°)$	$\varphi_E(°)$	$\varphi_B(°)$	x_B/λ_B	y_B/λ_B	$\theta^*(°)$
50.8764	23.5781	129.1235	-0.6309	0.7757	39.1235

Table 2. Design Parameters of the suggested exemple depend on the discretization

N	A_E/A_*	L/λ_B	C_{Mass}	C_F	ε (%)
3	13.09204	30.628	33.1919	1.2607	79.86
10	3.152120	7.8534	8.3765	0.5529	16.35
50	2.718915	6.8608	7.2917	0.5268	3.02
100	2.676870	6.7644	7.1862	0.5239	1.49
200	2.656574	6.7179	7.1353	0.5225	0.74
500	2.644610	6.6905	7.1053	0.5216	0.29
1000	2.640656	6.6815	7.0954	0.5213	0.14
5000	2.637505	6.6742	7.0875	0.5210	0.02
10000	2.637112	6.6733	7.0865	0.5210	0.01
20000	2.636915	6.6729	7.0860	0.5210	$7.45\ 10^{-3}$
50000	2.636797	6.6726	7.0857	0.5210	$2.98\ 10^{-3}$
100000	2.636758	6.6725	7.0856	0.5210	$1.49\ 10^{-3}$
200000	2.636738	6.6725	7.0855	0.5210	$7.45\ 10^{-4}$
500000	2.636726	6.6724	7.0855	0.5210	$2.98\ 10^{-4}$
1000000	2.636722	6.6724	7.0855	0.5210	$1.49\ 10^{-4}$
2000000	2.636720	6.6724	7.0855	0.5210	$7.45\ 10^{-5}$
3000000	2.636720	6.6724	7.0855	0.5210	$4.96\ 10^{-5}$
4000000	2.636719	6.6724	7.0855	0.5210	$3.72\ 10^{-5}$
5000000	2.636718	6.6724	7.0855	0.5210	$2.98\ 10^{-5}$
10000000	2.636718	6.6724	7.0855	0.5210	$1.49\ 10^{-5}$

$$\varepsilon_{parameter}\,\% = \left| 1 - \frac{Parameter_{\,Theoretical}}{Parameter_{\,Computed}} \right| \times 100 \tag{33}$$

We note that if the value of N increases, the ratio of the sections and the other parameters *converge in a decreasing way*, i.e. the computed value is always superior to the theoretical one. The o*ther ratios mentioned in table 2 converge towards the precise solution before the convergence of the sections ratio*, which is an advantage, in order to control only the convergence of the sections ratio.

The error given for each selected discretization is presented in Table 2. For $N=1000$ points, the error is less than 0.15%,and for $N=10000$ points the error is $\varepsilon=0.01\%$. We notice according to the obtained results, that for two discretizations of same values of M_E and γ, we can check this equality.

$$N_2/N_1 \approx \varepsilon_1/\varepsilon_2 \tag{34}$$

The results in Table 3 show the minimum number N of points required to obtain a specified error ε for the indicated exit Mach number M_E when $\gamma=1.40$. In Table 4, the effect of the specific heats ratio on the minimum number of points of the discretization error ε is shown. The minimum number of points N for the specified error depends on the values of M_E and γ.

Table 3. Minimum number of points N giving the error ε for $\gamma=1.40$

	$\varepsilon=0.1$	$\varepsilon=0.01$	$\varepsilon=0.001$	$\varepsilon=0.0001$	$\varepsilon=0.00001$
$M_E=1.5$	136	1349	13481	134803	1347936
$M_E=2.0$	621	6205	62040	620391	6203134
$M_E=3.0$	2706	27052	270515	2705097	27046001
$M_E=4.0$	5909	59094	590939	5909278	58973000
$M_E=5.0$	9789	97901	979028	9790076	97873419

Table 4. Minimum number of points N giving the error ε for $M_E=3.00$

	$\varepsilon=0.1$	$\varepsilon=0.01$	$\varepsilon=0.001$	$\varepsilon=0.0001$	$\varepsilon=0.00001$
$\gamma=1.30$	3296	32959	329584	3295767	32950902
$\gamma=5/3$	1814	18138	181380	1813769	18134834

Effect of the gas on the contour of the central body

Figures 8, 9, 10, 11, and 12 shown the contour of the central body for M_E=1.50, 2.00, 3.00 4.00, and 5.00. In theses figures, the nozzles are not confounded in the same point at the throat, considering the angle Ψ is not the same one. These points are on a circle of radius $\lambda_B=1.00$.

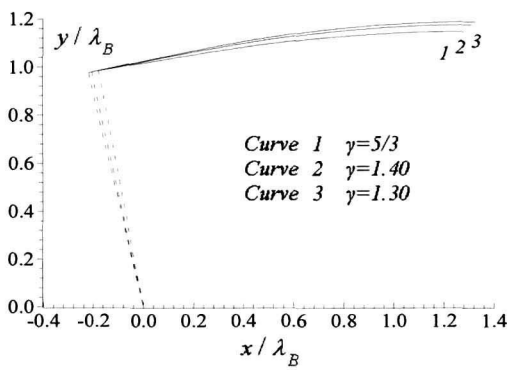

Fig. 8. Shapes of the plug nozzle when $M_E=1.50$

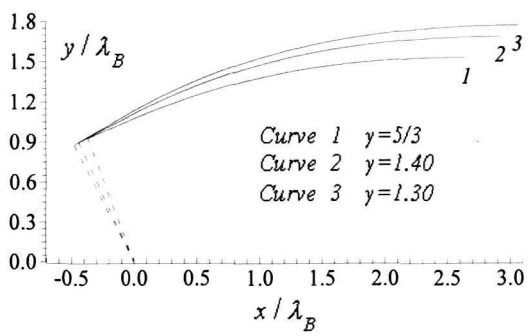

Fig. 9. Shapes of the plug nozzle when $M_E=2.00$

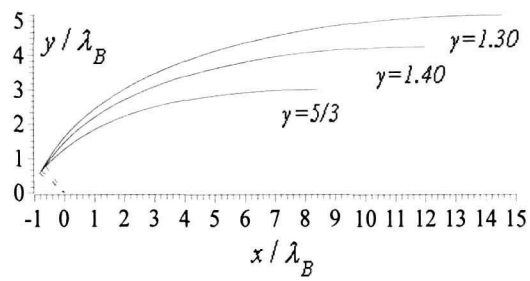

Fig. 10. Shapes of the plug nozzle when $M_E=3.00$

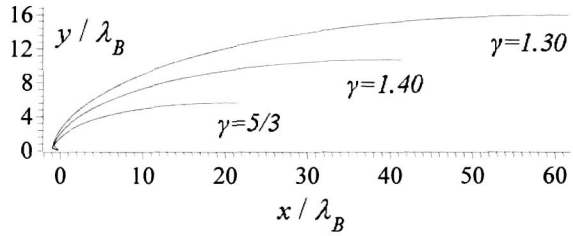

Fig. 11. Shapes of the plug nozzle when $M_E=4.00$

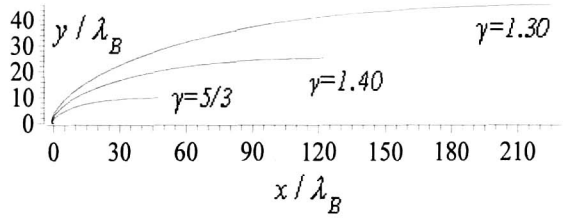

Fig. 12. Shapes of the plug nozzle when $M_E=5.00$

Variation of the parameters along the wall of the central body

Figures 13 and 14 present the variation of the Mach number and the flow deviation angle along the wall of the central body for various values of M_E when $\gamma=1.40$. The expansion of the gas due to increase of Mach number and a straightening of flow from the angle θ^* at the throat to $\theta=0$ at the exit can be seen.

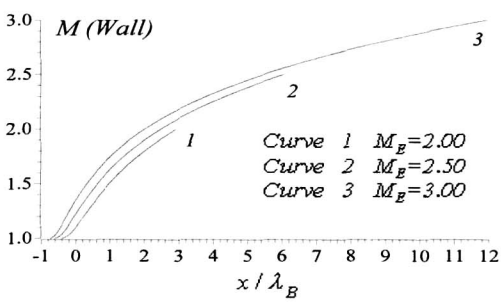

Fig. 13. Variation of the Mach number along the plug nozzle wall for air with $\gamma=1.40$

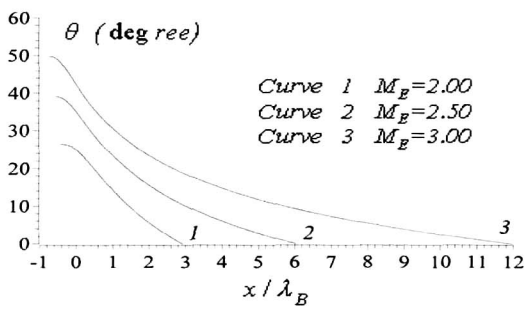

Fig. 14. Variation of the flow deviation angle along the plug nozzle wall for air with $\gamma=1.40$

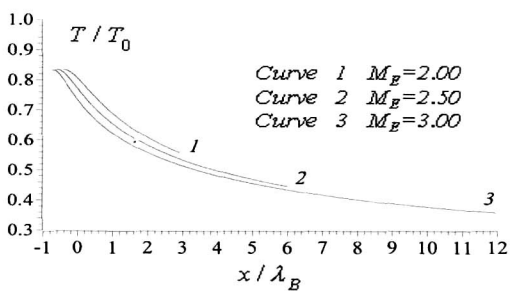

Fig. 15. Variation of the temperature ratio along the plug nozzle wall for air with $\gamma=1.40$

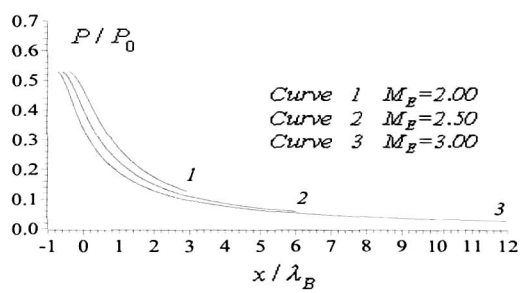

Fig. 16. Variation of the pressure ratio along the plug nozzle wall for air with $\gamma=1.40$

The figures 15 and 16 presents respectively the variation of the temperature and pressure raios along the wall of the central boty. The aim for the presentation of the temperature ratio is to make a suitable choice of the material building of the central body structure wich resist to this distribution. We note here again that the distribution of the temperature present also the bounady condition of the heat transefer problem in the material structure.

For the presentation of the pressure ratio, we can determine the pressure froce exerted on the wall of the central body and to make the calcul of the constraint and stress applied on the material building of the central body.

Variation of the design parameters

Figure 17 present the variation of the distance between the exit section and the lip (point *A*) versus the exit Mach number. The aim for the calculation of this distance is to have a sonic flow at the throat, and consequently a supersonic flow in the divergent part. *We note here that, if is this distance is not taken into account, we will have a subsonic flow at the col and consequenlty a subsonic flow in the divergent part.*

Figure 18 shows the variation of the central body length versus exit Mach number. On Figures 19, 20, 21, 22, 23, and 24, we respectively present the variation of the mass of the structure, the deviation of the lip relative to the vertical, the flow deviation angle at the throat, the pressure force exercted on the wall of the central body, the variation of the mass of gas and the exit section radius according to the exit Mach number.

We note that if we want to design a nozzle for missile applications having the smallest possible length and therfore having a small mass of the structure, it is necessary to choose *a gas having a smallest possible ratio* γ. In this case; the produced pressure force will be large. For the application of blowers, we make the design on the basis to obtain the smallest

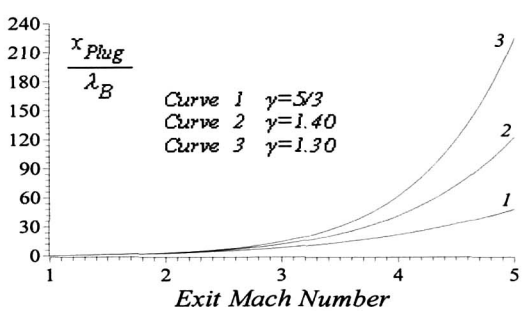

Fig. 17. Variation of the non-dimensional length of the nozzle versus exit Mach number

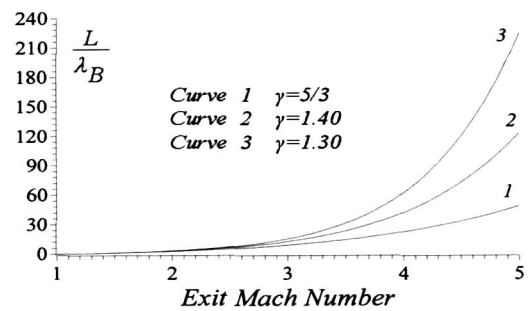

Fig. 18. Variation of the non-dimensional length of the nozzle versus exit Mach number

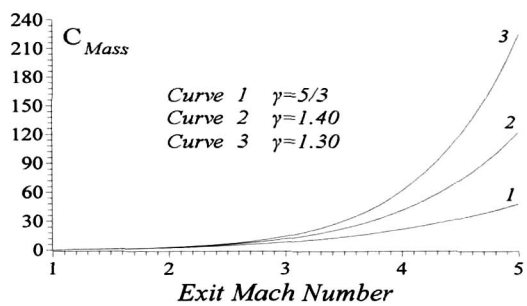

Fig. 19. Variation of the non-dimensional mass of the nozzle versus exit Mach number

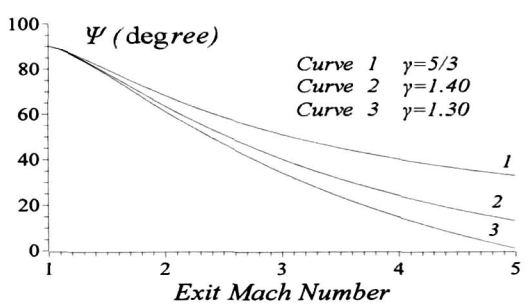

Fig. 20. Variation of the deviation angle of the lip versus exit Mach number

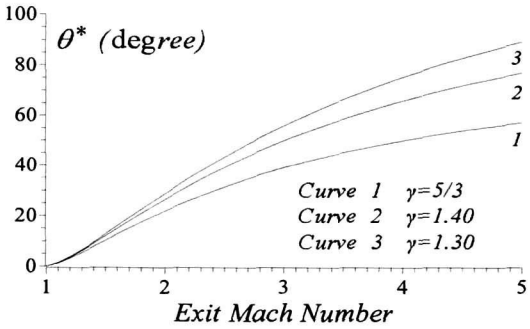

Fig. 21. Variation of the flow deviation angle at the throat versus exit Mach number

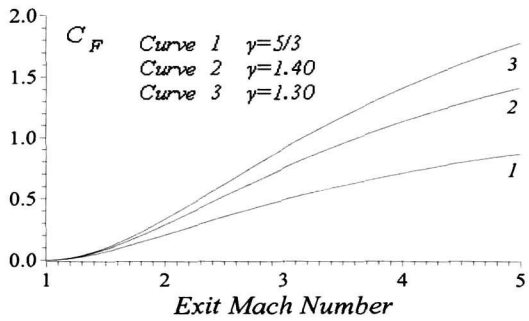

Fig. 22. Variation of the non-dimensional pressure force versus exit Mach number

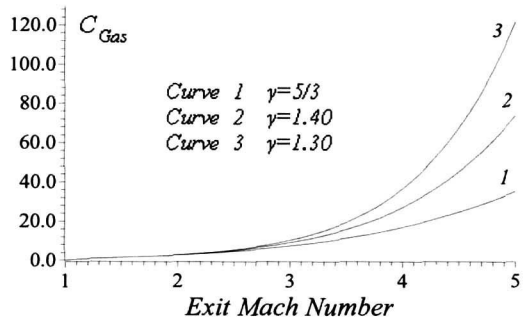

Fig. 23. Variation of the non-dimensional mass of the gas versus exit Mach number

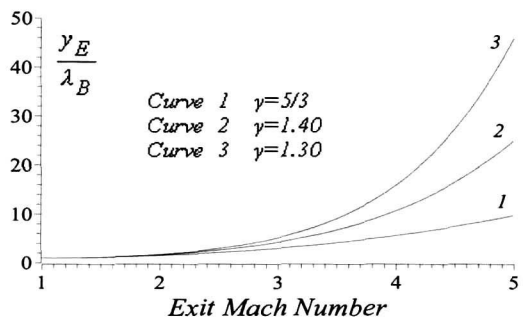

Fig. 24. Variation of the non-dimensional ray of the exit section versus exit Mach number

possible temperature at the exit section, to not to destroy the measuring instruments, and to save the ambient conditions, and to have possible largest ray of the exit section for the site of instruments. F*or the blowers, we are interested to use a gas having possible largest value of ratio* γ. We can deduce these results starting from relation (13) and isentropic temperature ratio[1].

Comparison of the plug nozzle and *MLN*

In Figure 25, the contours of plug nozzle and the Minimum Length Nozzle when $M_E=2.50$ and $\gamma=1.40$ are compared. We note that the plug nozzle has a smaller length and thus the mass compared to *MLN. The two nozzles deliver the same exit Mach number*, since they have the same exit section. The numerical values of comparison for this exemple are presented in Table 5. The values concern the *MLN* configuration can be found in refered 1) and 3).

Figure 26 compares the lengths of the two nozzles versus exit Mach number, Figure 27 for the mass of the structure and Figure 28 for the pressure force. For $M_E=2.50$ the improvements in length, mass of the structure and the pressure force are respectively 26%, 24%, and 55%. The flow field inside the plug nozzle is divided into a zone of transition *ABE* (simple region) and a zone of a uniform flow, which is not the case for the *MLN* that has in more non simple flow zone named by zone of Kernel.

Table 5. Calculation **results of the nozzle of figure 25**

	$\theta^*(°)$	$L/(dis)$	C_{Mass}	C_F
Plug Nozzle	*39.1235*	*6.6724*	*7.0855*	*0.5210*
MLN Nozzle	*19.6086*	*9.2241*	*9.3763*	*0.2367*

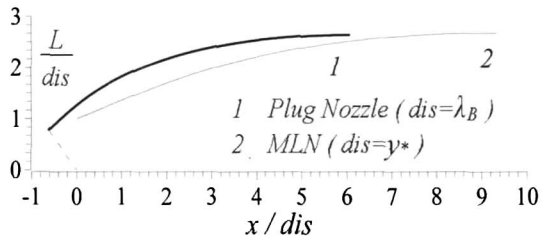

Fig. 25. Comparison between the plug nozzle and the *MLN* shapes for $M_E=2.50$ and $\gamma=1.40$

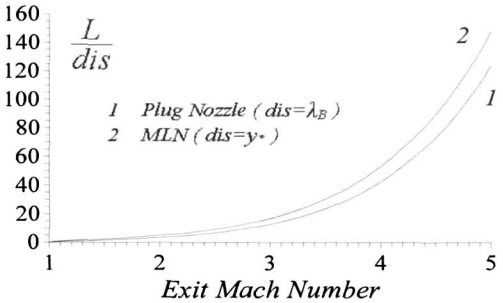

Fig. 26. Comparison between the length of the plug nozzle and *MLN* for the air

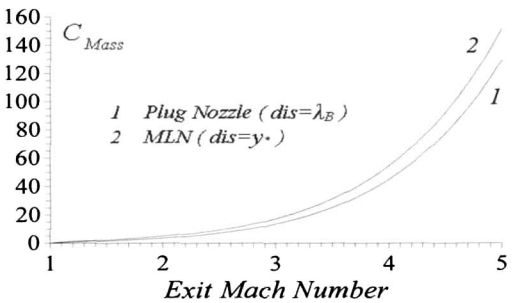

Fig. 27. Comparison between the mass of the structure of the plug nozzle and *MLN* for the air

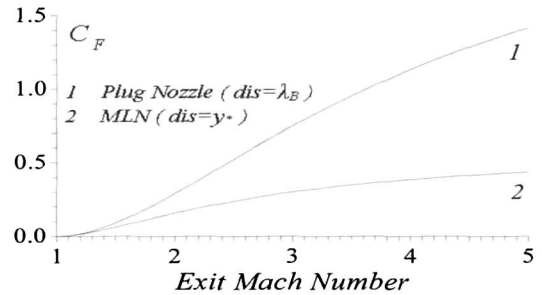

Fig. 28. Comparison between the pressure force of the plug nozzle and the *MLN* for the air

Conclusion

From this study, we can quote the following points:

We have illustrated an improvement for the supersonic nozzle parameters compared to the *MLN* configuration, which is often used in the aeronautical applications, by new shape of nozzle called plug nozzle.

As the flow at the exit is horizontal, we can truncate the nozzle at a section having an angle of deviation one or two degree, and in this case we will gain a very interesting portion of the mass. The flow at the exit of the truncated nozzle is not horizontal on the level of the wall and in this case we will loose a little of the produced pressure force. We note here that if the author accepts a truncation of the nozzle at a section having a rather large deviation of the flow which can reach to 5 or 6 degree, we can still gain mass of the structure but in parallel, we will loose a little of the pressure force delivered by the nozzle. The whole study can be made in this idea.

The developed method can make the design until an error of $\varepsilon=10^{-6}$, in a very reduced time through the discretization requires a high number of points. The design method is based on the Mach number.

The calculation and the determination of the contour of the central body depends not on the positioning choice of the reference mark considering the nozzle is two-dimensional.

The more the Mach waves number N is large, the more we obtain a very good presentation of the central body.

The determination of the points of the wall is done in an explicit way. If we know the position and the properties of a point on the wall, we can easily determine those of the adjacent point on the right until we reach the exit section point.

The point A of a lip is a discontinuity point of properties M and θ ... etc.

The authors like to thank the authorities of the University of Blida and the Department of Aeronautics for financial support for conducting this research. The authors acknowledge *Djamel ZEBBICHE* for granting time to prepare this manuscript.

References

1. Shapiro A. H., "C*ompressible Fluid Flow, "* Vol. 1, New York, the Ronald Press, 1953.

2. Hill P. G. and Peterson C.R., "*Mechanical and Thermodynamics of Propulsion*", Addition-Wesley Publishing Company Inc., New York, 1965.

3. J. D. Anderson Jr., "*Modern Compressible Flow. With Historical Pers pective*", 2nd ed. Mc Graw-Hill Book Company, New York, 1982.

4. J. D. Anderson Jr., "*Fundamentals of* Aerodynamics", 2nd ed., Mc Graw-Hill Book Company, New York, 1988.

5. Rao G.V.R., "Recent Developments in Rocket Nozzle Configuration", ARS Journal, Nov., 1961, pp. 1488, 1494.

6. Michael F. and Robert H., "Performance aspects of plug cluster nozzles", Journal of Spacecraft And Rockets, Vol. 33, No. 4, 1996, pp. 507, 512.

7. Rommel T., Hagemann G., Schley C. A., Kruelle G., and Manski D., "Plug Nozzle Flowfield Analysis", Journal of Propulsion and Power, Vol. 13, No. 5, 1997, pp. 629, 634.

8. Francesco N. and Marcello, O., "Methodology to Solve Flowfields of Plug Nozzles for Future Launchers", Journal of Propulsion and Power, Vol. 14, No. 3, 1998, pp. 318, 326.

9. Gerald H., Hans I., Thong V.N., and Gennady E. D., "Advanced Rocket Nozzles", Journal of Propulsion and Power, Vol. 14, No. 5, 1998, pp. 620, 634.

10. Francesco N. and Marcello O., "Theoretical Analysis and Engineering Modeling of Flowfields in Clustered Module Plug Nozzles", Journal of Propulsion and Power, Vol. 15, No. 4, 1999, pp. 544, 551.

11. Korte J. J., Salas A. O., Dunn H. J., Alexandrov N. M., Follett W. W., Orient G. E. and Hadid A. H., "Multidisciplinary Approach to Linear Aerospike Nozzle Design", Journal of Propulsion and Power, Vol. 17, No. 1, 2001, pp. 93, 98.

12. Kraiko A. N., Tillyayeva N. I. and Baftalovskii S. .V, "Optimal Design of Plug Nozzles and Their Thrust Determination at Start", Journal of Propulsion and Power, Vol. 17, No. 6, 2001, pp. 1347, 1352.

13. Takashi I., Fujii K., Hayashi A. K., "Computations of Axisymmetric Plug-Nozzle Flowfields: Flow Structures and Thrust Performance", Journal of Propulsion and Power, Vol. 18, No. 2, 2002, p. 254-260.

14. Menko E. N. W. and Willem J. B., "Trailing-Edge Cavity Afterbodies for Linear Plug Nozzle Engines", AIAA Journal, Vol. 41, No. 9,2003, pp. 1715, 1721.

15. Hagemann G., Immich H. and Terhardt M., "Flow phenomena in advanced rocket nozzles - The plug nozzle", AIAA-1998-3522, 34th AIAA/ASME/SAE/ASEE Joint Propulsion Conference and Exhibit, Cleveland, OH, July 13-15, 1998.

16. Marsilio R., "Numerical simulations for plug nozzle flowfield", AIAA-2001-670, 39th Aerospace Sciences Meeting and Exhibit, Reno, NV, Jan. 8-11, 2001.

17. Zebbiche T., "Supersonic Plug Nozzle Design,"AIAA-2005-4490, 41th AIAA/ASME/SAE/ASEE Joint Propulsion Conference and Exhibit, Arizona, July 10-13, 2005.

18. Onofri M., "CFD Results of Plug Nozzle Test Cases", AIAA-2002-4036, 38th AIAA/ASME/SAE/ASEE Joint Propulsion Conference and Exhibit, Indianapolis, Indiana, July 7-10, 2002.

19. Wisse M., van Oudheusden B. and Bannink W., "Analytical Optimisation of an Inviscid Flow Linear Plug Nozzle Boattail", AIAA-2004-4017, 40th AIAA/ASME/SAE/ASEE Joint Propulsion Conference and Exhibit, Fort Lauderdale, Florida, July 11-14, 2004.

20. Greer, H., "Rapid Method for Plug Nozzle Design", ARS Journal, April 1961, pp. 560-561.

21. Angelino, G., "Approximate Method for Plug Nozzle Design", AIAA Journal, Vol. 2, N° 10, 1964, pp. 1834-1835.

22. Rao, G. V. R., "Spike Nozzle Contour for Optimum Thrust", Ballistic Missile and Space Technology, edited by C. W. Morrow, Vol. 2, Pergamon Press, New York, 1961, pp. 92-101.